Balancing of thermal lenses in enhancement cavities with transmissive elements

N. Lilienfein,[1,2,*] H. Carstens,[1,2] S. Holzberger,[1,2] C. Jocher,[3] T. Eidam,[3] J. Limpert,[3] A. Tünnermann,[3] A. Apolonski,[1,2] F. Krausz,[1,2] and I. Pupeza[1,2]

[1]*Max-Planck-Institut für Quantenoptik, Hans-Kopfermann-Str. 1, 85748 Garching, Germany*

[2]*Ludwig-Maximilians-Universität München, Fakultät für Physik, Am Coulombwall 1, 85748 Garching, Germany*

[3]*Friedrich-Schiller-Universität Jena, Institut für Angewandte Physik, Albert-Einstein-Str. 15, 07745 Jena, Germany*

**Corresponding author: nikolai.lilienfein@mpq.mpg.de*

Received December 5, 2014; accepted January 19, 2015;
posted January 22, 2015 (Doc. ID 229074); published February 27, 2015

Thermal lensing poses a serious challenge for the power scaling of enhancement cavities, in particular when these contain transmissive elements. We demonstrate the compensation of the lensing induced by thermal deformations of the cavity mirrors with the thermal lensing in a thin Brewster plate. Using forced convection to fine-tune the lensing in the plate, we achieve average powers of up to 160 kW for 250-MHz-repetition-rate picosecond pulses with a power-independent mode size. Furthermore, we show that the susceptibility of the cavity mode size to thermal lensing allows highly sensitive absorption measurements.

OCIS codes: (140.4780) Optical resonators; (140.7240) UV, EUV, and X-ray lasers.
http://dx.doi.org/10.1364/OL.40.000843

In high-finesse passive optical resonators, the pulses of a mode-locked laser can be coherently stacked to achieve a power enhancement of several orders of magnitude. Such enhancement cavities (ECs) are powerful tools for driving frequency conversion processes exhibiting low single-pass efficiencies such as high-order harmonic generation (HHG) in gaseous media [1,2] or inverse Compton scattering from relativistic electrons [3,4] at high repetition rates. Another promising application of this generic concept has been the "stack and dump" approach, where a stretched femtosecond pulse circulating in the EC is periodically dumped after having built up to allow for high pulse energies while almost maintaining the high input average power [5,6]. In the resonant state, high-finesse ECs exhibit an enhanced sensitivity towards changes of their longitudinal and transverse field distributions, making them uniquely sensitive measurement tools for application fields ranging from gravitational-wave detection [7] over molecular spectroscopy [8], to the measurement of linear [9] and nonlinear [10] polarization response of materials.

Together with intensity-related damages, thermal effects in the cavity optics ultimately limit the achievable intracavity peak and average power. In a previous work [11], we demonstrated the enhancement of ultrashort pulses to average powers of several hundreds of kilowatts. To avoid intensity-induced damage, large spot sizes on the mirrors are necessary. This can be conveniently achieved at an alignment-insensitive edge of the resonator stability zone [12]. Even though the dielectric mirrors employed in [11] were carefully chosen to minimize susceptibility to thermal lensing, at hundreds of kilowatts of average power, the transverse cavity mode was significantly affected by thermally induced changes. Many high-power applications require transmissive elements in the beam path of the EC, rendering thermal lensing an even more serious challenge. For instance, in cavity-enhanced HHG Brewster plates [13] or anti-reflection-coated plates placed at grazing incidence [14] can be used to couple out the generated radiation. Another example are nonlinear conversion processes in intracavity crystals, such as terahertz generation [15], intrapulse difference-frequency generation [16], or spectral broadening via self-phase modulation [17,18].

In this Letter, we experimentally and theoretically investigate thermally-induced changes in the size of the modes of high-finesse cavities containing transmissive elements. We show that the optics of an EC can be chosen such that the thermally-induced phase-front distortions largely compensate for each other. To precisely balance the contribution of a thin plate with those of the mirrors, we demonstrate a technique to fine-tune its thermal lensing characteristics. With this method, we achieve an intracavity average power of 160 kW in an EC containing a fused silica Brewster plate (BP), while drastically reducing thermally induced changes of the mode size. The susceptibility of the mode size to thermal lenses allows for measurements of total absorptions of thin transmissive plates in the range of 0.1 ppm.

The concept of combining optics with different dependencies of dioptric power on temperature to athermalize imaging systems has been used since the 1940s [19]. Later, this approach was used to mitigate self-induced thermal lensing of the gain medium in laser resonators [20–22], focusing optics for laser machining [23], and other high-power laser optics [24,25]. In ECs, such compensation has to be achieved at average powers of hundreds of kilowatts, which is orders of magnitude higher than in previous applications of the concept.

Thermal lensing of mirrors is caused by absorption of the incident power P in the coatings. The resulting thermal expansion of the substrate deforms the mirror surface, causing it to act as a defocusing optical element upon reflection. The thermally-induced radius of curvature R_{ref1} scales as [26]

$$R_{\mathrm{ref1}}^{-1} \propto -\frac{\alpha A}{\kappa w^2} \cdot P, \tag{1}$$

with the absorption coefficient of the coating A, the thermal conductivity κ and thermal expansion coefficient α of

the substrate, and the $1/e^2$ intensity radius w of the incident beam. By using coatings with an absorption of a few ppm and low-expansion glass substrates, thermal deformations can be alleviated [11]. However, the high bulk absorption of low-expansion glasses prevents their use as substrates for input couplers of ECs [11]. Thus, thermal lensing in state-of-the-art all-reflective ECs is dominated by the surface deformation of the input coupler.

In transmissive elements, thermal lensing effects are caused by absorption in the bulk material as well as in coatings. The resulting temperature distribution also leads to surface deformations, but usually their effect is negligible compared to the phase front distortions caused by the temperature-dependence of the refractive index dn/dT. The lensing effect scales as [27]

$$R_{\mathrm{trans}}^{-1} \propto \frac{al}{\kappa w^2}\frac{dn}{dT}\cdot P, \tag{2}$$

with l being the thickness and a the absorption coefficient of the element. In most materials the temperature coefficient of the refractive index is positive, resulting in focusing thermal lenses. Because of the low temperatures and thermal gradients seen in the experiments, we neglect the dependence of the thermal conductivity on temperature, and stress-induced effects.

To understand how focusing and defocusing thermal phase front distortions affect a resonator, it is useful to distinguish between their parabolic and higher-order content. Purely parabolic phase front distortions act as perfect lenses altering the focusing geometry of the cavity and, thus, its position in the stability zone. This changes the mode size and can lead to configurations where higher order transverse modes are degenerate with the fundamental mode [28]. The dependence of the mode size on the focusing geometry diverges at the edges of the stability zone. To avoid mirror damage, the EC can be operated close to the inner edge of stability, where the illuminated areas on the mirrors are increased [12]. Here, a defocusing thermal lens pushes the cavity further towards the edge. Additionally, all transverse modes with even orders converge at this edge of stability [28]. The higher order content of thermal phase front distortions facilitates coupling of the fundamental transverse mode to higher order modes, causing losses [11]. These effects make a precise compensation of both thermal lensing and aberrations desirable. Conversely, the susceptibility of high-finesse cavities to thermal effects can be exploited to measure small absorptions with a high sensitivity [29,30].

We simulated the deformation of the input coupler caused by the absorption of a Gaussian beam using the finite-element solver COMSOL. Figure 1 shows the phase front distortion produced by a beam of 100 kW on a mirror with a coating of 5 ppm absorption and a fused-silica substrate. Heat exchange with the ambience is assumed to take place only via radiation, with the emissivity of the mirror being 0.95. A parabolic fit to this profile, weighted with the incident intensity profile, yields its dioptric power. The residuals of this fit represent aberrations. We find that a thin fused-silica plate placed in a collimated arm of the cavity is well suited to compensate for the thermal aberrations of the input coupler (Fig. 1). The

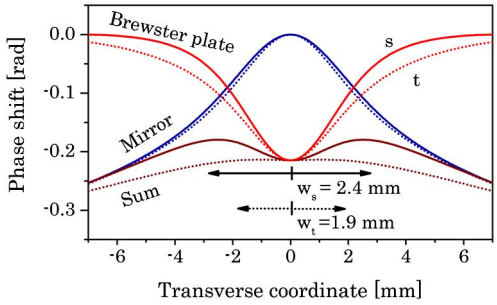

Fig. 1. Simulated thermal phase distortion profiles induced by an elliptical Gaussian beam. Profiles are plotted for a mirror, a Brewster plate, and their sum in both the sagittal (s, solid lines) and tangential planes (t, dotted lines).

plate is placed at Brewster's angle to minimize losses and to avoid additional absorption in anti-reflection coatings [Fig. 2(a)]. The projection of a round beam on the plate is then an ellipse, with the ratio of its major to its minor axis being about 1.76. This leads to astigmatism of the thermal lens, with the shorter focal length in the plane of the tilt.

Because of the different shapes of the heating patterns on the input coupler and on the BP, their thermal lenses cannot be perfectly matched in the sagittal and tangential planes simultaneously [Fig. 1]. Thus, the ellipticity of the cavity mode will change with intracavity power. For a cavity close to the inner edge of the stability zone with non-zero angles of incidence on the curved mirrors, the mode is elliptical in the cold state. Its major axis lies in the sagittal plane of the mirrors. By placing the BP such that the tilt angle is within this plane, its astigmatic thermal lensing behavior can be exploited to compensate for the initial ellipticity at a given intracavity power.

To model the thermal sensitivity of a specific cavity design, we use the metric introduced in [11], given by the slope of the beam radius on a curved mirror as a function of the intracavity average power. Close to the inner edge of the stability zone the mode change evolves nearly linear with the intracavity power, making this metric a useful tool to estimate the behavior of the cavity even for high powers [11]. First, we calculate the mode size in both planes for the cold, i.e., low-power cavity. Next, we simulate the heating of the input coupler and of the BP by this beam for a small power in 3D using COMSOL

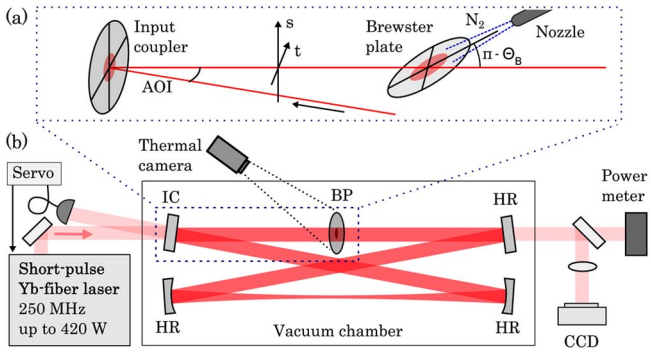

Fig. 2. (a) Sketch of the compensation scheme. The Brewster plate (BP) is tilted in the sagittal plane. The minimal angle of incidence (AOI) depends on the distance between input coupler (IC) and BP, and the mode size. The plate can be cooled with nitrogen gas. (b) Schematic of the experimental setup.

and extract the resulting phase distortion profiles (Fig. 1). From these we obtain the sagittal and tangential focusing powers of the thermal lenses by a parabolic fit, weighted with the incident intensity profile. By plugging the resulting thermal lenses into the cavity model, we calculate the mode size of the warm cavity and its thermal sensitivity. In Fig. 3, a the thermal sensitivity of a symmetric 2.4-m bow-tie cavity is plotted against the initial mode size. The simulations were performed for cavity configurations close to the inner stability edge, with the positions in the stability zone corresponding to the initial mode size [Fig. 3(a)].

In the experiment, we use a four-mirror cavity seeded by the Yb:fiber-based chirped-pulse-amplification laser system published in [31]. It delivers 250-fs pulses centered at 1040 nm with a repetition rate of 250 MHz and up to 420 W of average power. The pulses were stretched to about ten picoseconds for the experiments to exclude nonlinear effects. The laser is locked to the EC using the Pound-Drever-Hall scheme. The cavity comprises three high-reflectance mirrors with ultra-low-expansion glass substrates and an input coupler with a reflectivity of 99.85% on a fused-silica substrate, and is placed in a vacuum chamber [Fig. 2(b)]. It is set up in a symmetric bow-tie geometry [12] with two 600-mm radius-of-curvature mirrors. The distance between the curved mirrors can be varied to adjust the position in the stability zone. We use a round BP made of fused silica (Suprasil 311, Heraeus), with a diameter of 25 mm and a thickness of 100 μm. To avoid clipping the cavity beam while minimizing the angles of incidence on the mirrors, the BP is placed as indicated in Fig. 2. To determine the thermal sensitivity of the cavity, the mode profile on one of the curved mirrors was measured for a range of intra-cavity powers using the same diagnostics as described in [11]. The obtained data was fitted by a linear function. The thermal sensitivity is given by the slope of the fit function, and the initial mode size corresponds to its value at zero power [Fig. 3(b)]. Measurement series were performed with and without the BP for different cavity configurations close to the inner stability edge [Fig. 3(a)].

The model can be fitted to the experimental results by using the absorptions of the input coupler and of the BP as free parameters. For absorption values of 3.2 ppm in the mirror and 0.28 ppm in the plate, theory and experiment show excellent agreement [Fig. 3(a)]. The measurements allow distinguishing absorptions with a resolution of about 0.5 ppm in mirrors and 0.02 ppm in BPs. With the Brewster plate, a clean, round mode is achieved at 62 kW with a power enhancement factor of 1300. The experiments demonstrate that the astigmatism of the thermal lens from the BP can be used to eliminate the initial mode ellipticity. Still, the thermal sensitivity differs significantly from zero, meaning that the balancing of thermal lenses is not perfect [Fig. 3(b)].

In principle, a good compensation is achievable by precisely choosing the thickness of the BP. However, the manufacturing tolerance and availability of plates, as well as small changes in the surface absorption of individual plates in between experiments, make this approach impractical. To overcome this problem, we exploit the high surface-to-volume ratio of the thin BP. It allows for an efficient manipulation of the amount of heat emitted within the illuminated area, and thus of the strength of the thermal lens. This can be achieved by changing the ambient temperature apparent to the plate, or by facilitating heat transport through a gas. Here, we expose a BP of 200 μm thickness to forced convection by directing a steady flow of nitrogen along its surface [Fig. 2(a)]. This method offers a broad range of tunability [Fig. 4(a)]. With this scheme, we achieve an intracavity average power of 160 kW, i.e., with an enhancement factor of 1035, and a nearly constant mode size [Fig. 4(a)]. At this power, losses from thermally induced aberrations prevent further scaling [Fig. 4(b)]. These aberrations seem to stem primarily from the inhomogeneous cooling of the BP [Fig. 4(c)–4(e)], resulting in a significant tilt of

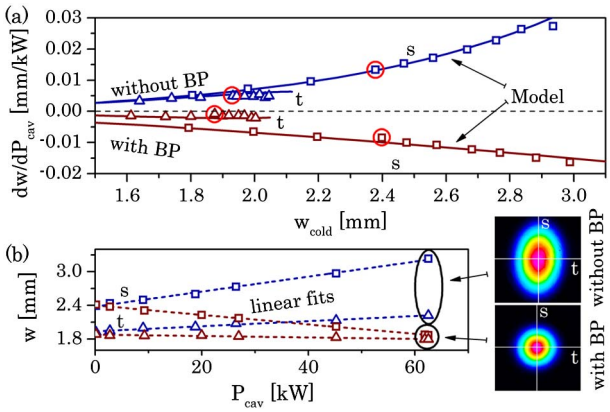

Fig. 3. (a) Thermal sensitivity plotted versus the initial mode size in both the sagittal (s, squares) and tangential (t, triangles) plane. The model (solid lines) agrees well with the experimental results (symbols). The points marked by red circles are derived from the data shown in (b). (b) Beam radius versus intracavity power with and without a Brewster plate (BP) (symbols) and linear fits (dashed lines). Beam profiles are shown for both cases at an intracavity power of 61 kW.

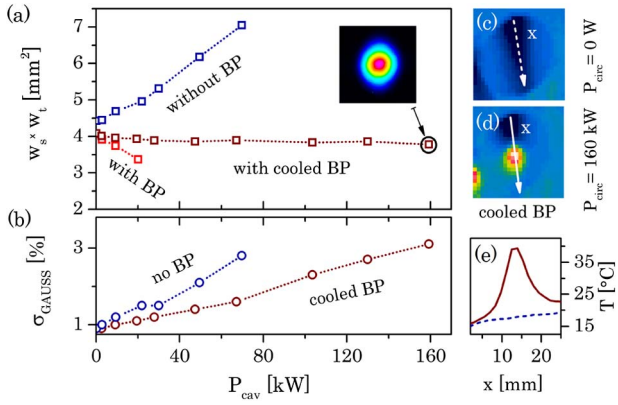

Fig. 4. (a) Mode area versus intracavity power for the same cavity without a Brewster plate, with an uncooled and with a cooled Brewster plate. The inset shows a mode profile achieved with the cooled BP at 160 kW. (b) Standard deviation of the Gaussian fit to the mode profile in the sagittal plane, indicating increasing aberrations. (c),(d) Images of the temperature distribution on the cooled Brewster plate for two powers. The arrow indicates the direction of the cooling gas flow. (e) Temperature profiles on the Brewster plate along the arrows exhibit a significant asymmetry of the thermal lens.

the temperature profile in the sagittal plane, which becomes more severe with increasing power. This technological limitation can in principle be overcome by improving the cooling of the BP. A promising alternative to forced convection could be radiative cooling [32].

In conclusion, we have investigated the enhancement of ultrashort pulses in a high-finesse EC containing a transmissive element. We have demonstrated that the thermal lenses induced in the cavity mirrors and in a thin plate placed at Brewster's angle in the beam path can be balanced with high precision by controlling forced convection of the plate. We have also shown that thermal lensing in BPs can be exploited to compensate for astigmatism in cavities operated close to the edge of stability. With this scheme, we obtained a constant mode size up to 160 kW of average power, which exceeds the performance of state-of-the-art ECs with transmissive elements by more than one order of magnitude. Furthermore, we show that the sensitivity of the cavity mode change with respect to the thermal lens induced in thin plates allows for the detection of absorption values in the range of ~0.1 ppm. The methodology applied in this work will benefit the power scaling of ECs, in particular for applications requiring the inclusion of transmissive elements like nonlinear crystals or output couplers for radiation generated via intracavity conversion processes.

We thank Johannes Weitenberg for helpful discussions. This work was supported by the Deutsche Forschungsgemeinschaft (DFG) Cluster of Excellence, Munich Centre for Advanced Photonics (MAP), by the Bundesministerium für Bildung und Forschung (BMBF) under Photonische Nanomaterialien (PhoNa), contract number 03IS2101B, by the Fraunhofer-Max Planck project MEGAS, and by the European Research Council under the ERC grant agreement no. [617173] ACOPS.

References

1. C. Gohle, T. Udem, M. Herrmann, J. Rauschenberger, R. Holzwarth, H. A. Schuessler, F. Krausz, and T. W. Hänsch, Nature **436**, 234 (2005).
2. I. Pupeza, S. Holzberger, T. Eidam, H. Carstens, D. Esser, J. Weitenberg, P. Rußbüldt, J. Rauschenberger, J. Limpert, T. Udem, A. Tünnermann, T. W. Hänsch, A. Apolonski, F. Krausz, and E. Fill, Nat. Photonics **7**, 608 (2013).
3. Z. Huang and R. Ruth, Phys. Rev. Lett. **80**, 976 (1998).
4. J. Bonis, R. Chiche, R. Cizeron, M. Cohen, E. Cormier, P. Cornebise, N. Delerue, R. Flaminio, D. Jehanno, F. Labaye, M. Lacroix, R. Marie, B. Mercier, C. Michel, Y. Peinaud, L. Pinard, C. Prevost, V. Soskov, A. Variola, and F. Zomer, J. Inst. **7**, P01017 (2012).
5. Y. Vidne, M. Rosenbluh, and T. W. Hansch, Opt. Lett. **28**, 2396 (2003).
6. S. Breitkopf, T. Eidam, A. Klenke, L. von Grafenstein, H. Carstens, S. Holzberger, E. Fill, T. Schreiber, F. Krausz, A. Tünnermann, I. Pupeza, and J. Limpert, Light Sci. Appl. **3**, e211 (2014).
7. G. M. Harry, Class. Quantum Grav. **27**, 84006 (2010).
8. F. Adler, M. J. Thorpe, K. C. Cossel, and J. Ye, Annu. Rev. Anal. Chem. **3**, 175 (2010).
9. I. Pupeza, X. Gu, E. Fill, T. Eidam, J. Limpert, A. Tünnermann, F. Krausz, and T. Udem, Opt. Express **18**, 26184 (2010).
10. S. Holzberger, N. Lilienfein, H. Carstens, T. Saule, F. Lücking, M. Trubetskov, V. Pervak, T. Eidam, J. Limpert, A. Tünnermann, E. Fill, F. Krausz, and I. Pupeza are preparing a manuscript to be called "Femtosecond enhancement cavities in the nonlinear regime."
11. H. Carstens, N. Lilienfein, S. Holzberger, C. Jocher, T. Eidam, J. Limpert, A. Tünnermann, J. Weitenberg, D. C. Yost, A. Alghamdi, Z. Alahmed, A. Azzeer, A. Apolonski, E. Fill, F. Krausz, and I. Pupeza, Opt. Lett. **39**, 2595 (2014).
12. H. Carstens, S. Holzberger, J. Kaster, J. Weitenberg, V. Pervak, A. Apolonski, E. Fill, F. Krausz, and I. Pupeza, Opt. Express **21**, 11606 (2013).
13. C. Benko, T. K. Allison, A. Cingöz, L. Hua, F. Labaye, D. C. Yost, and J. Ye, Nat. Photonics **8**, 530 (2014).
14. O. Pronin, V. Pervak, E. Fill, J. Rauschenberger, F. Krausz, and A. Apolonski, Opt. Express **19**, 10232 (2011).
15. M. Theuer, D. Molter, K. Maki, C. Otani, J. A. L'huillier, and R. Beigang, Appl. Phys. Lett. **93**, 41119 (2008).
16. I. Pupeza, D. Sánchez, J. Zhang, N. Lilienfein, M. Seidel, O. Pronin, N. Karpowicz, T. Paasch-Colberg, I. Znakovskaya, V. Pervak, E. Fill, Z. Wei, F. Krausz, A. Apolonski, and J. Biegert are preparing a manuscript to be called "High-power sub-2-cycle mid-infrared pulses at 100 MHz repetition rate."
17. K. D. Moll, R. J. Jones, and J. Ye, Opt. Express **13**, 1672 (2005).
18. V. L. Kalashnikov, Appl. Phys. B **92**, 19 (2008).
19. J. W. Perry, Proc. Phys. Soc. London **55**, 257 (1943).
20. N. P. Barnes and D. J. Gettemy, J. Opt. Soc. Am. **70**, 1244 (1980).
21. R. Koch, Opt. Commun. **140**, 158 (1997).
22. E. Wyss, M. Roth, T. Graf, and H. P. Weber, IEEE J. Quantum Electron. **38**, 1620 (2002).
23. M. Scaggs and G. Haas, Proc. SPIE **7913**, 79130C (2011).
24. S. Piehler, C. Thiel, A. Voss, M. Abdou Ahmed, T. Graf, E. Beyer, and T. Morris, Proc. SPIE **8239**, 82390Z (2012).
25. M. Stubenvoll, B. Schäfer, and K. Mann, Opt. Express **22**, 25385 (2014).
26. W. Winkler, K. Danzmann, A. Rüdiger, and R. Schilling, Phys. Rev. A **44**, 7022 (1991).
27. J. P. Gordon, R. C. C. Leite, R. S. Moore, S. P. S. Porto, and J. R. Whinnery, J. Appl. Phys. **36**, 3 (1965).
28. J. Weitenberg, P. Rußbüldt, I. Pupeza, T. Udem, H.-D. Hoffmann, and R. Poprawe, "Geometrical on-axis access to high-finesse resonators by quasi-imaging: a theoretical description," J. Opt. (to be published).
29. S. Hild, H. Lück, W. Winkler, K. Strain, H. Grote, J. Smith, M. Malec, M. Hewitson, B. Willke, J. Hough, and K. Danzmann, Appl. Opt. **45**, 7269 (2006).
30. N. Lastzka, J. Steinlechner, S. Steinlechner, and R. Schnabel, Appl. Opt. **49**, 5391 (2010).
31. C. Jocher, T. Eidam, S. Hädrich, J. Limpert, and A. Tünnermann, Opt. Lett. **37**, 4407 (2012).
32. C. Justin Kamp, H. Kawamura, R. Passaquieti, and R. DeSalvo, Nucl. Instrum. Methods Phys. A **607**, 530 (2009).